



REPORT

Localized inshore warming, acidification, and elevated particulate organic matter across a coupled mangrove, seagrass, and coral reef ecosystem in La Parguera, Puerto Rico

Carla L. Mejias-Rivera¹ · Roy A. Armstrong¹ · Sawyer Balint² · Erick García-Troche¹ · Richard A. McKinney² · Julio M. Morell³ · Autumn Oczkowski² · Travis A. Courtney¹

Received: 14 March 2023 / Accepted: 2 October 2023 / Published online: 21 October 2023
© The Author(s), under exclusive licence to International Coral Reef Society (ICRS) 2023

Abstract Global declines in mangroves, seagrasses, and corals threaten the provisioning of ecosystem services to coastal communities. However, potential feedbacks between these ecosystems are poorly understood owing to a lack of studies exploring functional links between these frequently coupled nearshore tropical ecosystems. To better understand these links, we sampled seawater temperature, salinity, and pH in addition to particulate organic carbon, particulate organic nitrogen, and their respective stable isotope composition ($\delta^{13}\text{C}$ and $\delta^{15}\text{N}$) monthly from July 2018 to June 2019 at sites ranging from inshore to offshore in La Parguera Natural Reserve, Puerto Rico. We observed persistent, year-round warmer, more acidic, and higher particulate organic matter seawater at the most inshore Bioluminescent Bay station compared to sites further offshore. Particulate organic carbon values ranged from a maximum of 764 mg/m^3 at the most inshore station to a minimum of 53.96 mg/m^3 at the most offshore station while particulate organic nitrogen ranged from 166 mg/m^3 at the most inshore station to 6.39 mg/m^3 at the most offshore station. Biogeochemical variability across spatial scales largely followed gradients in biological and physical controls, with limited differences between the more offshore coral reef sites and the most intense biogeochemical modification occurring in the shallowest and most nearshore stations. Limited temporal variability was observed for most parameters except for seasonal variations

in temperature, salinity, and pH. Particulate organic matter stable isotope composition were slightly enriched at inshore stations and suggested a mixture of primarily marine allochthonous and autochthonous organic matter sources. The importance of heterotrophy for coral resilience to warming and acidification suggests this localized nutrition-rich albeit warmer and acidified waters in nearshore mangrove and seagrass ecosystems is an important functional link to nearshore corals with the potential to modulate coral resilience to ocean warming and acidification.

Keywords Acidification · Coral reef · Mangrove · Particulate organic matter · Seagrass · Stable isotopes

Introduction

Mangrove, seagrass, and coral reef ecosystems provide myriad direct and indirect benefits to over 1.3 billion people living in tropical coastal communities worldwide (Moberg and Folke 1999; Harborne et al. 2006; Sale et al. 2014; United Nations 2021). These ecosystems often co-occur along tropical coastal shorelines and provide benefits both individually and synergistically as a result of the important abiotic and functional linkages between them (Harborne et al. 2006). For example, the combination of mangroves, seagrasses, and coral reefs provide greater shoreline protection than when only one or two of these ecosystems are present (Guannel et al. 2016). Despite the importance of these ecosystems to the stability of the environment, coastal communities, and the economy, human activities have been negatively impacting the Earth system's balance since the Industrial Revolution resulting in widespread degradation of marine ecosystems (Hoegh-Guldberg and Bruno 2010). Global increases in anthropogenic CO_2 are causing warming of the upper

✉ Carla L. Mejias-Rivera
carla.mejias@upr.edu

¹ Department of Marine Sciences, University of Puerto Rico Mayagüez, Mayagüez, PR, USA

² Environmental Protection Agency Atlantic Coastal Environmental Sciences Division, Narragansett, RI, USA

³ Caribbean Coastal Ocean Observing System (CARICOOS), Lajas, PR, USA

ocean layers, ocean acidification (OA), and deoxygenation (Diaz 2001; Doney 2010; Arias et al. 2021) and these global changes are compounded by local anthropogenic stressors (Ryan et al. 2008; García-Sais et al. 2021). Consequently, tropical coastal ecosystems are in decline as evidenced by a 20% decline in mangroves from 1980 to 2005 (FAO 2007), a 29% decline in seagrass beds from 1879 to 2006 (Waycott et al. 2009), and a 50% decline in coral cover from 1957 to 2007 (Eddy et al. 2021).

Reef-building corals have been particularly susceptible to ocean warming with bleaching-induced coral mortality observed for 35% of surveyed corals in the 2014–2017 marine heat waves alone (Eakin et al. 2022). Coral bleaching is the breakdown of symbiosis between the host coral and symbiotic algae, which can provide up to 100% of the daily metabolic carbon needs for the host coral (Hatcher 1988). Healthy “non-bleached” corals typically derive 15–35% of their daily metabolic needs from heterotrophy by direct capture of dissolved or particulate organic matter, but this number can be up to 100% in bleached corals when corals no longer have their symbiotic algae to provide nutrition (Houlbrèque and Ferrier-Pagès 2009). Heterotrophy is therefore a potential buffer against rising temperatures by providing additional energy to enable coral resistance to marine heat waves and facilitate recovery from coral bleaching events (Rezende et al. 1990; Grottoli et al. 2006; Sippo et al. 2017). Adequate nutrition also appears to maintain coral growth rates under reduced pH conditions projected for near future ocean acidification (Towle et al. 2015; Ramajo et al. 2016; Courtney et al. 2017). However, coral reefs are typically present in nutrition-poor regions of the world’s oceans suggesting the supply of nutrition to coral reefs may become increasingly important for maintaining resilient coral-dominated ecosystems under ongoing ocean warming and acidification (Goreau et al. 1971; Alldredge et al. 2013; Duarte et al. 2013).

Odum’s “outwelling hypothesis” proposed that organic material exuded from nearshore environments such as mangroves and seagrasses may supply and sustain the growth of offshore coral reef ecosystems through the delivery of nutrition and therefore may represent an important functional link between mangroves, seagrasses, and corals (Odum 1968; Odum et al. 1979; Lee 1995; Sippo et al. 2017; Santos et al. 2021). This horizontal transport of outwelled nutrition may occur via the direct export of dissolved or particulate matter (e.g., planktonic, terrestrial, and microbial particles), animal migration, or through predator–prey interactions (Bouillon and Connolly 2009; Cruz and Neuer 2019; Kharbush et al. 2020). The quantity of outwelled organic matter typically varies due to source availability, coastal geomorphology, geophysics, and hydrodynamics as well as land hydrologic features, temperature, precipitation, and inundation regimes (Robertson et al. 1984; Bianchi and Bauer 2011; Cael and

Follows 2016). Upwelling, recycling, remineralization, and seasonally variable offshore productivity have all been hypothesized as additionally important sources of organic matter to coral reef systems (Williams et al. 2012; Alldredge et al. 2013; Duarte et al. 2013; Ducklow and Doney 2013; Yeakel et al. 2015; Kealoha et al. 2019; Courtney et al. 2020).

Stable isotopes of particulate organic carbon ($\delta^{13}\text{C}$) and nitrogen ($\delta^{15}\text{N}$) may provide information on the various sources of organic matter, trophic pathways, ecosystem dynamics, and material or nutrient transport between ecosystems and species (Rodelli et al. 1984; Lee 1995; Anderson and Fourqurean 2003; Lamb and Swart 2008; Oczkowski et al. 2014, 2016, 2018) owing to differential isotope fractionation during biogeochemical processes (Dawson and Brooks 2001; Brain 2006). For example, $\delta^{13}\text{C}$ from terrestrial plants typically range from -10 to -16‰ for plants with C4 metabolic pathways (e.g., saltmarsh vegetation) and -21 to -32‰ for plants with C3 metabolic pathways (e.g., mangroves) (Lamb et al. 2006, and references therein). On the other hand, marine particulate organic carbon typically ranges from -18 to -24‰ , bacteria from -12 to -27‰ , algae and seagrass from -16 to -24‰ , and dissolved organic carbon from -22 to -25‰ (Lamb et al. 2006, and references therein). The use of $\delta^{15}\text{N}$ and C:N ratios provide additional information to help discriminate among converging ranges of $\delta^{13}\text{C}$ (Anderson and Fourqurean 2003; Lamb and Swart 2008; Oczkowski et al. 2014).

In this study, we focused on quantifying temperature, pH, and particulate organic matter at sites ranging from inshore to offshore from mangroves and seagrasses to a nearshore coral reef system in order to better understand potentially important functional linkages between these tropical coastal ecosystems. While we focused here on particulate organic matter as a key source of potential coral nutrition in the context of this study, we acknowledge that dissolved organic matter represents an additional potential source of coral nutrition not captured by this study (Houlbrèque and Ferrier-Pagès 2009). To accomplish this task, we characterized the spatial and temporal variability of temperature, salinity, pH, particulate organic carbon (POC) and nitrogen (PON), and particulate organic carbon ($\delta^{13}\text{C}$) and nitrogen ($\delta^{15}\text{N}$) isotope ratios at four distinct sites ranging from inshore to offshore and separated by multiple spatial scales in La Parguera Natural Reserve (LPNR). LPNR is an optimal location to study functional linkages between mangroves, seagrasses, and coral reefs because of the proximity of these ecosystems across an inshore–offshore gradient. Specifically, we addressed the following question: What is the seasonal and inshore–offshore variability in seawater temperature, salinity, pH, POC, PON, $\delta^{13}\text{C}$, and $\delta^{15}\text{N}$ in LPNR? This multi-ecosystem perspective provides new insights into the functional links between coupled coastal ecosystems and how

tradeoffs between changes in temperature, pH, and available nutrition may influence the resilience of nearshore coral reefs under climate change.

Methods

Study area

The study was conducted in LPNR, an approximately 11-km-wide embayment located in southwest Puerto Rico in the Caribbean Sea (Fig. 1). The Natural Reserve includes coastal mangroves, lagoonal and nearshore seagrasses, a series of coral reef cays scattered across an inner shelf averaging ~6 m depth, and foreereef development that extends out to the shelf edge at ~18–20 m depth (Morelock et al. 1977). LPNR is characterized by a wet season from August to November, spring showers normally during April and May, and typically dry conditions over the remaining months of the year (Margalef 1961; Vega Rodríguez and Aponte 2008; García-Troche et al. 2021; Ayala-Torres 2022). The area has no direct riverine inputs and models for this watershed estimate that submarine groundwater discharge represents 10% (range = 0–12%) of the total surface runoff (Luijendijk et al. 2020). Seasonal freshwater inputs from the Amazon and Orinoco Rivers are correlated with reductions in seawater salinity and may also deliver nutrients to the area (Corredor and Morell 2001). Since 2011, the increasing influx of *Sargassum* spp. seaweeds and related sargassum brown tides have been contributing to the organic material deposited in the coastal waters of La Parguera (Wang et al. 2019; Hernández et al. 2022; Pérez-Pérez 2022; León-Pérez et al. 2023).

Four study sites were chosen along an inshore to off-shore gradient in LPNR, including mangrove, seagrass, and coral reef ecosystems with varying influences of terrestrial and oceanic processes (Fig. 1). The Bioluminescent Bay (BB) of LPNR was selected as the most inshore station (Fig. 1C). This shallow embayment has an average depth of 3.5 m with a maximum depth of approximately 4.5 m. A fringing *Rhizophora mangle* mangrove forest separates the bay from contiguous salt flats (Soler-Figueroa and Otero 2015), and the benthos is dominated by muddy sediments and areas of *Thalassia testudinum* and *Halophila baillonis* seagrasses (Almodovar and Blomquist 1959). Cayo Enrique (NQ) is the next station moving offshore and consists of a lagoonal back reef region that reaches depths of approximately 4 m (Fig. 1B). This station is predominantly composed of *Thalassia testudinum* seagrass beds interspersed in calcareous and sandy sediments (Morelock et al. 1977; Zayas-Santiago 2011). The Acidification Buoy (AB) station is located approximately 150 m further offshore and across the foreereef from the Cayo Enrique station (Fig. 1B). The Acidification Buoy (NOAA PMEL MAPCO2 Buoy) rests in an area where the total depth is approximately 6 m and the benthic coverage includes a variety of hard corals (10–11%), octocorals (26%), macroalgae and turf (17%), carbonate sands, rubble, and rock (35%), and other (11%) (Hernández-López 2015; Meléndez et al. 2022). The Veril (VL) station is located furthest away from the shoreline (approximately 12 km offshore) near the shelf edge. The shelf edge is located at approximately 18–25 m depths and is dominated by a long band of a submerged reef with an average scleractinian coral cover of 39% (Todd et al. 2009; Sherman et al. 2016).

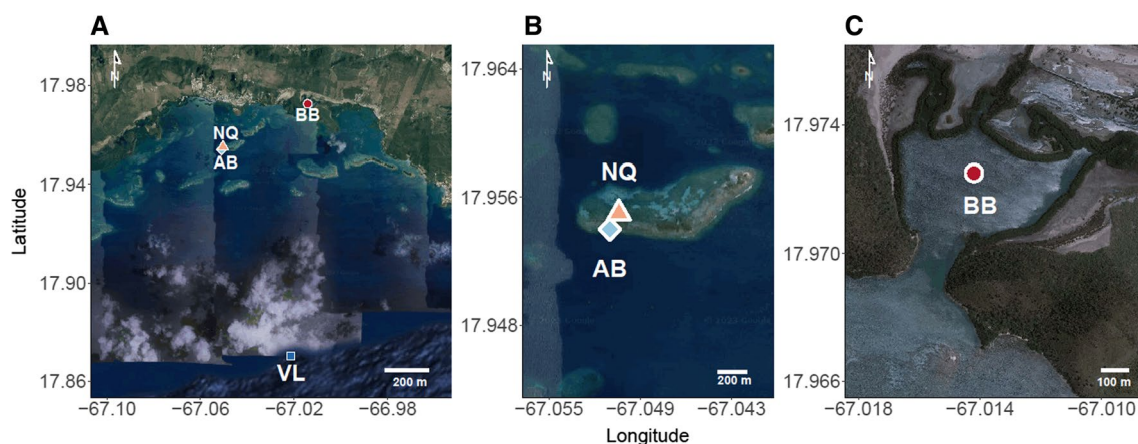


Fig. 1 Map of sampling stations at La Parguera Natural Reserve (LPNR), Southwest Puerto Rico. The red circle labeled “BB” indicates the Bioluminescent Bay sampling station, the orange triangle labeled “NQ” indicates the Cayo Enrique sampling station, the light blue diamond labeled “AB” indicates the Acidification Buoy sampling station, and the dark blue square labeled “VL” indicates the

Veril sampling station. Panel A shows the broader LPNR with all four sampling stations, panel B shows just the Cayo Enrique and Acidification Buoy sampling stations separated by the reef crest of Cayo Enrique, and panel C shows the Bioluminescent Bay and adjacent salt flats

Sample collection, management, and analysis

Seawater surveys were conducted during the morning hours (08:00–12:00 AST) approximately monthly from July 2018 to June 2019 for temperature (T), salinity (S), pH, particulate organic carbon (POC), particulate organic nitrogen (PON), particulate organic carbon isotope ratio ($\delta^{13}\text{C}$), and particulate organic nitrogen isotope ratio ($\delta^{15}\text{N}$). Throughout this study, we have collected primarily surface seawater samples following the canonical assumption that coral reef seawaters are well-mixed and therefore provide a general characterization of the respective site, but note that water column processes can be increasingly important relative to benthic processes at sites with deeper depths (e.g., Veril Station) and can result in detectable vertical gradients of seawater biogeochemistry (Long et al. 2019; Pezner et al. 2021). Temperature and salinity were measured in situ at 1 m depth via a SBE 25 Sealogger CTD from SeaBird Scientific with a SBE 3F sensor (accuracy: ± 0.0002 °C) for temperature and a SBE 4C sensor (accuracy: ± 0.0003 S/m) for salinity. Precipitation data for the years 2018 and 2019 were obtained from the NOAA NCDC database (<https://www.ncdc.noaa.gov/cdo-web/>) and the cumulative sum for 2 weeks prior to each sampling date was calculated using the runner package in R (Kałedkowski 2023). Water samples for pH were collected at slightly deeper depths of 3 m for BB, 1.5 m for NQ, and 4 m for AB and VL to leverage concurrent sampling efforts by the CARICOOS Ocean Acidification Project. These samples were collected according to standard practices (Dickson et al. 2007) and analyzed by spectrophotometry on the Total Scale using a double-beam Shimadzu spectrophotometer with m-cresol purple indicator dye (precision: ± 0.006) at the Isla Magueyes Field Station, University of Puerto Rico Mayagüez, as previously described (Meléndez et al. 2020).

Seawater was sampled for particulate organic matter (POC, PON, $\delta^{13}\text{C}$, $\delta^{15}\text{N}$) in triplicate at 1 m depth using a 5 L Van Dorn bottle. Two Van Dorn bottle casts were necessary to fill three 3.8 L Nalgene carboys to ensure adequate sample volumes for each triplicate. Water samples were filtered the same day upon arrival at the laboratory, with the filtrate volume quantified via a graduated cylinder. Each sample was vacuum-filtered through a previously combusted 25-mm-diameter GFF filter, dried in a muffle furnace at 65°C overnight, acidified overnight with HCl fumes for inorganic carbon removal, and redried at 65°C overnight for excess acid removal following Joint Global Ocean Flux Study (JGOFS) protocols (Knap et al. 1996; Mishonov et al. 2003; Chaves et al. 2020).

Analysis for the elemental and stable isotope composition of particulate organic matter (POC, PON, $\delta^{13}\text{C}$, $\delta^{15}\text{N}$) was performed using a continuous flow isotope ratio mass spectrometer (Isoprime 100) interfaced with an elemental analyzer (Micro Vario, Elementar Americas, Mt. Laurel,

New Jersey, USA) at the United States Environmental Protection Agency Atlantic Coastal Environmental Sciences Division, Rhode Island, USA. Replicate analyses of internationally recognized isotope standard reference materials USGS40 ($\delta^{13}\text{C} = -26.4\text{‰}$, $\delta^{15}\text{N} = -4.5\text{‰}$) and USGS41 ($\delta^{13}\text{C} = +37.6\text{‰}$, $\delta^{15}\text{N} = +46.6\text{‰}$) were used to calibrate an in-house working standard (blue mussel homogenate, $\delta^{13}\text{C} = -18.3\text{‰}$, $\delta^{15}\text{N} = +11.2\text{‰}$), which was used to normalize isotope results to air ($\delta^{15}\text{N}$) and Vienna Pee Dee Belemnite ($\delta^{13}\text{C}$) scales (Paul et al. 2007; Oczkowski et al. 2016). The elemental composition of the sample was calculated by comparing the peak area of the sample to a standard curve of peak area vs elemental composition of standard reference material Cystine (%C = 30.0%, %N = 11.7%). POC and PON were then converted to concentrations (mg/m^3) via the mass (mg) divided by the respective filtered volume (L) for each sample. Isotope ratios are expressed in δ (‰) notation calculated by the following formula:

$$X(\text{permil}) = \left[\left(\frac{R_{\text{sample}}}{R_{\text{reference}}} \right) - 1 \right] * 1000$$

where $X = {}^{13}\text{C}$ when $R = {}^{13}\text{C}/{}^{12}\text{C}$ and, similarly, $X = {}^{15}\text{N}$ when $R = {}^{15}\text{N}/{}^{14}\text{N}$.

Quality assurance and quality control of particulate organic matter (POC, PON, $\delta^{13}\text{C}$, $\delta^{15}\text{N}$) results were based on the variance of triplicate measurements. We flagged all triplicates that had a high variance or were outliers relative to the entire dataset for additional review as determined by Tukey's fences following internal protocols developed by the Environmental Protection Agency laboratory. Of these flagged samples, only single measurements that exhibited clear signs of sample contamination relative to the other triplicates were removed from subsequent analyses (i.e., 0.7% of the individual replicates; see supplemental information for R script for all removed triplicates and the rationale for their removal). The resulting mean standard deviation for our particulate organic matter measurements is ± 27 mg/m^3 for POC, ± 3 mg/m^3 for PON, $\pm 0.8\text{‰}$ for $\delta^{13}\text{C}$, and $\pm 1\text{‰}$ $\delta^{15}\text{N}$.

Data processing and statistical analysis

We used ANOVA to test for detectable differences in temperature, salinity, pH, POC, PON, $\delta^{13}\text{C}$, $\delta^{15}\text{N}$, and C:N between sites and months. Site and Month were used as fixed effect predictors for each of the respective measured parameters following a stepwise Akaike information criterion (AIC) approach that tested increasingly complex models including the null model, Month-only model, Site-only model, Month and Site model, and the Month and Site and Interaction of Month and Site model. The model with the lowest AIC value was selected as the best model to fit the data and was qualitatively assessed for model assumptions

using the performance package (Lüdecke 2021). We then used p values and performed Tukey Honest Significant Difference tests for the lowest AIC model to evaluate pair-wise comparisons of the fixed effects and report detectable differences in the given measured parameter (i.e., temperature, salinity, pH, POC, PON, $\delta^{13}\text{C}$, $\delta^{15}\text{N}$, and C:N) between months or sites. To assess multidimensional differences in measured seawater parameters between sites and the co-varying seawater chemistry parameters responsible for driving detectable differences in seawater chemistry between sites, we also conducted a principal component analysis with 95% confidence ellipses. All data analyses were conducted using the R programming language (R Core Team 2022).

Results

Temporal and spatial variability in seawater parameters

Temperature

Seawater temperatures ranged from 26.23 to 30.24 °C throughout the year following a typical seasonal cycle in LPNR with the coolest seawater temperatures observed from January through March and the warmest temperatures observed from July through October (Fig. 2A) (see code for full pair-wise comparison of seawater temperature between months). Seawater temperatures generally decreased moving offshore with the lowest temperatures recorded at the Veril site compared to the Acidification Buoy ($p=0.019$), Cayo Enrique ($p<0.001$), and Bioluminescent Bay ($p<0.001$) sites (Fig. 3A). Similarly, lower temperatures were recorded at the Acidification Buoy site compared to the more inshore Cayo Enrique ($p=0.001$) and Bioluminescent Bay ($p<0.001$) sites. No temperature differences were detected

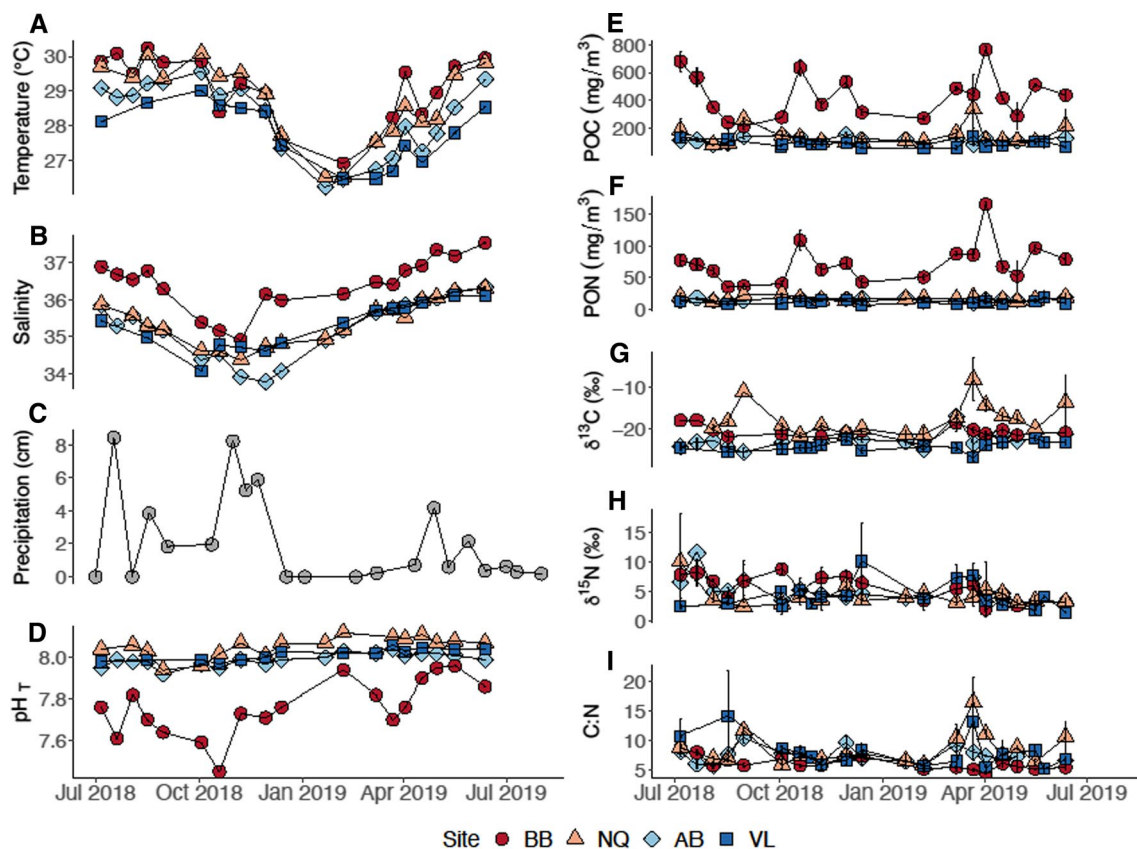


Fig. 2 Time series measurements from each parameter during the July 2018–June 2019 sampling period. Each data point represents a sampling event and data for POC, PON, $\delta^{13}\text{C}$, $\delta^{15}\text{N}$, and C:N represent the mean \pm standard deviation of replicate samples. Precipitation data reflect the 14-day cumulative sum prior to each sampling

event (gray circle). Red circles labeled “BB” indicates the Bioluminescent Bay sampling station, orange triangles labeled “NQ” indicates the Cayo Enrique sampling station, light blue diamonds labeled “AB” indicate the Acidification Buoy sampling station, and dark blue squares labeled “VL” indicate the Veril sampling station

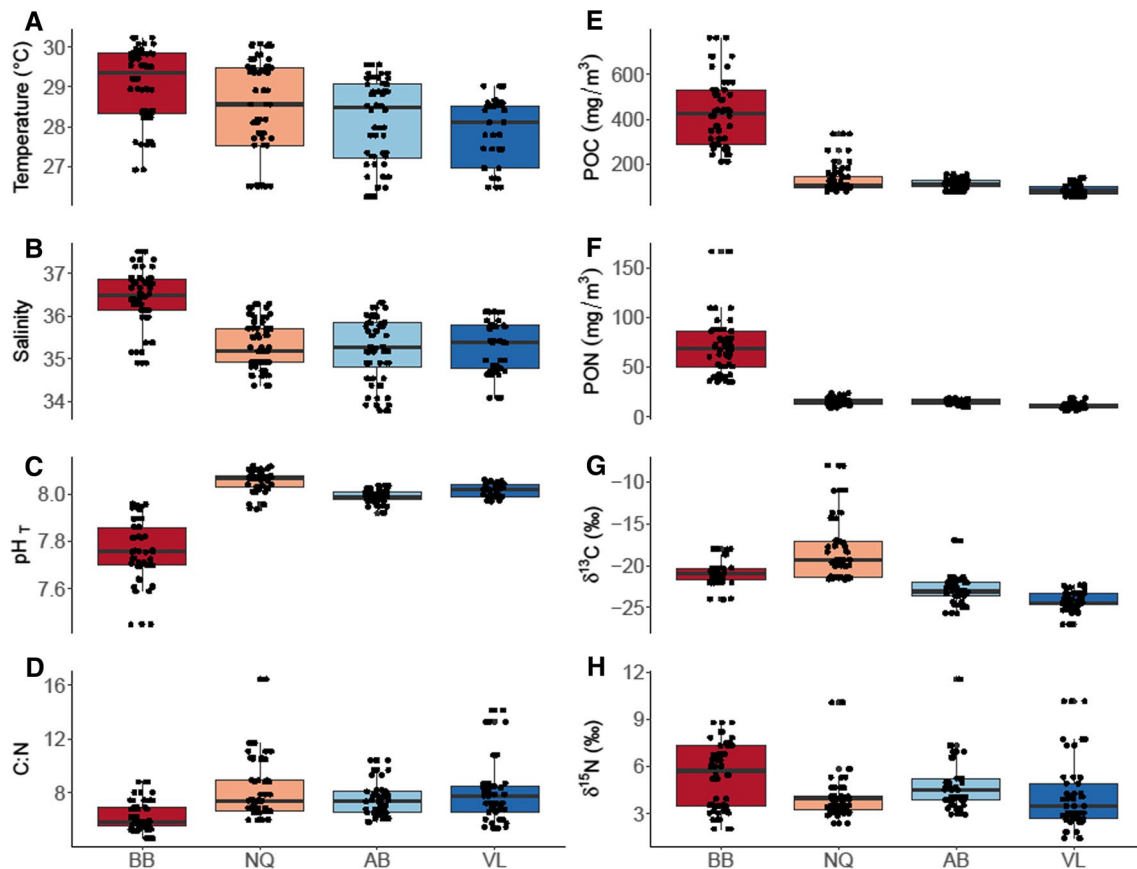


Fig. 3 Inshore to offshore site-level data for each measured parameter. The black line within the boxes represents the median, and the upper and lower hinges represent the first and third quartiles (25th and 75th percentiles), respectively. Jitter points for temperature, salinity and pH represent single sampling events while jitter points for POC,

PON, $\delta^{13}\text{C}$, $\delta^{15}\text{N}$, and C:N represent the triplicate mean for each sampling event. Stations are ordered from inshore to offshore, left to right where “BB” represents the Bioluminescent Bay station, “NQ” represents the Cayo Enrique station, “AB” represents the Acidification Buoy station, and “VL” represents the Veril station

Table 1 Summary statistics are reported for the best AIC model selected for each parameter

	Temperature	Salinity	pH	POC	PON	$\delta^{13}\text{C}$	$\delta^{15}\text{N}$	C:N
Site	<0.001	<0.001	<0.001	<0.001	<0.001	<0.001	0.011	0.006
Month	<0.001	<0.001	<0.001				<0.001	
Site × month							0.004	
Num.Obs	69	69	68	71	71	67	70	71
R ²	0.901	0.920	0.840	0.724	0.722	0.529	0.846	0.168
AIC	79.6	25.8	−170.1	845.1	602.4	312.8	254.2	307.0

“Site”, “Month”, and “Site × Month” represent the *p* values for the respective fixed effects for each biogeochemical parameter. “Num.Obs.” lists the number of observations evaluated for each model, “R²” represents the Coefficient of determination, and “AIC” represent the Akaike Information Criterion. Empty spaces represent cases where the respective fixed effects were not included in the best AIC model selected for each parameter. Please see the associated code release for statistical summaries and pair-wise comparisons of all model outputs

between Cayo Enrique and Bioluminescent Bay ($p=0.056$) (Fig. 3A). The additive site and month model was selected as the best model based on lowest AIC with detectable differences in measured temperature between months ($p<0.001$) and sites ($p<0.001$) (Table 1). There was no detectable interaction between site and month ($p=0.65$).

Salinity

Seawater salinities ranged from 33.79 to 37.52 throughout the year following a typical seasonal cycle in LPNR with the lowest salinities observed from October to December compared to higher salinities observed for the rest of the year (Fig. 2B) (see code for full pair-wise comparison of seawater salinity between months). Precipitation 14-day cumulative sum during the study period ranged from 0.00 to 8.41 cm of rain with higher rain events recorded in late summer and fall, limited precipitation during the winter months, and a slight increase in precipitation during the spring months (Fig. 2C). Lowest salinities coincided with highest precipitation months observed during the last quarter of the year (Fig. 2C). Seawater salinities were highest at the Bioluminescent Bay site compared to all other sites ($p<0.001$) (Fig. 3B). There were no detectable pair-wise differences in salinity between the Cayo Enrique, Acidification Buoy, and Veril sites ($p>0.05$). The additive site and month model was selected as the best model based on the lowest AIC with detectable differences in measured salinity among months ($p<0.001$) and sites ($p<0.001$) (Table 1). There was no detectable interaction between site and month on salinity ($p=0.562$).

pH

Seawater pH ranged from 7.45 to 8.12 with lower pH generally recorded in summer months and higher pH generally recorded in winter months (e.g., see code for full pair-wise comparison of seawater pH between months) (Fig. 2D). Seawater pH generally increased from inshore to offshore with lower pH recorded at the Bioluminescent Bay site compared to the Acidification Buoy ($p<0.001$), Cayo Enrique ($p<0.001$), and Veril ($p<0.001$) sites (Fig. 3C). Similarly, lower pH was recorded at the Acidification Buoy site compared to Cayo Enrique ($p=0.013$) with no detectable differences in pH between the Acidification Buoy and Veril sites ($p=0.626$) (Fig. 3C). The interaction model had the lowest AIC but there was no detectable interaction between site and month on pH ($p=0.172$). Therefore, the additive site and month model, which had the second lowest AIC value and significant predictors, was selected as the best model to fit the data with detectable differences in measured pH between months ($p<0.001$) and sites ($p<0.001$) (Table 1).

POC

Seawater POC generally decreased moving offshore and ranged from a maximum of 764.23 mg/m³ at the Bioluminescent Bay site to a minimum of 53.96 mg/m³ at the Veril Site with no clear temporal pattern (Figs. 2E, 3E). Higher POC was detected at the Bioluminescent Bay site compared to all other sites ($p<0.001$) (Fig. 3E). There were no detectable pair-wise differences in POC between the Acidification Buoy, Cayo Enrique, and Veril sites ($p>0.05$) (Fig. 3E). The site model was selected as the best model based on the lowest AIC with detectable differences in measured POC between sites ($p<0.001$) (Table 1). There was no detectable effect of month on POC ($p=0.93$) or detectable interaction between site and month on POC ($p=0.808$).

PON

Seawater PON generally decreased moving offshore and ranged from a maximum of 166.13 mg/m³ at the Bioluminescent Bay station to a minimum of 6.39 mg/m³ at the Veril station with no evident temporal pattern (Figs. 2F, 3F). Higher PON was detected at the Bioluminescent Bay site compared to all other sites ($p<0.001$) (Fig. 3F). There were no detectable pair-wise differences in PON between the Acidification Buoy, Cayo Enrique, and Veril sites ($p>0.05$) (Fig. 3F). The site model was selected as the best model based on the lowest AIC with detectable differences in measured PON between sites ($p<0.001$) (Table 1). There was no detectable effect of month ($p=0.993$) or interaction between site and month on PON ($p=0.968$).

$\delta^{13}C$

Seawater $\delta^{13}C$ generally decreased moving offshore and ranged from -27.0 to -8.0% with no evident temporal trend (Fig. 2G). Consistently enriched (higher) values were observed at the Cayo Enrique site, especially during spring and fall, compared to the Bioluminescent Bay ($p<0.01$), Acidification Buoy ($p<0.001$), and Veril ($p<0.001$) sites (Fig. 3G). The most deplete $\delta^{13}C$ were observed at the Veril site, which were also detectably more depleted (lower) than Bioluminescent Bay $\delta^{13}C$ ($p<0.001$). There were no detectable pair-wise differences in $\delta^{13}C$ between the Acidification Buoy, Bioluminescent Bay, and Veril sites ($p>0.05$). The site model was selected as the best model based on lowest AIC with detectable differences in $\delta^{13}C$ between sites ($p<0.001$) (Table 1). There was no detectable effect of month ($p=0.711$) or interaction between site and month on $\delta^{13}C$ ($p=0.439$).

$\delta^{15}\text{N}$

Seawater $\delta^{15}\text{N}$ generally decreased from inshore to offshore and ranged from 11.5 to 1.4‰ throughout the year with lower $\delta^{15}\text{N}$ generally recorded in winter months and higher $\delta^{15}\text{N}$ generally recorded in summer months (e.g., see code for full pair-wise comparison of seawater $\delta^{15}\text{N}$ between months) (Fig. 2H). Higher $\delta^{15}\text{N}$ values were observed at the Bioluminescent Bay site compared to the Cayo Enrique and Veril sites ($p < 0.05$) but were not detectably different from the Acidification Buoy site ($p > 0.05$) (Fig. 3H). There were no detectable pair-wise differences in $\delta^{15}\text{N}$ between the Cayo Enrique, Acidification Buoy, and Veril sites ($p > 0.05$). The additive month, site, and interaction model was selected as the best model based on lowest AIC with detectable differences in measured $\delta^{15}\text{N}$ between sites ($p = 0.011$), months ($p < 0.001$), and the interaction between site and month ($p < 0.01$) (Table 1).

C:N

Seawater C:N ranged from 4.59 to 16.46 throughout the year with no evident temporal trend (e.g., see code for full pair-wise comparison of seawater C:N between months) (Fig. 2I). Higher values were observed at the Cayo Enrique site, compared to the Bioluminescent Bay ($p < 0.01$), but were not detectably different from the Acidification Buoy

and Veril sites ($p > 0.05$) (Fig. 3D). There were no detectable pair-wise differences in C:N between the Acidification Buoy, Bioluminescent Bay, and Veril sites ($p > 0.05$). The additive site and month model had the lowest AIC but there were no detectable differences between months ($p = 0.06$). Therefore, the site model which had the second next lowest AIC was selected as the best model to fit the data with detectable differences in measured C:N between sites ($p < 0.01$), (Table 1).

Principal component analysis and covariation between seawater parameters

Principal component analysis (PCA) further revealed detectable differences between the depth, precipitation, and the biogeochemistry sampled at the Bioluminescent Bay site compared to the Cayo Enrique, Acidification Buoy, and Veril sites (Fig. 4). These differences were primarily driven by the first principal component (PC1), which explained 35% of the total variance and differentiated the Bioluminescent Bay site based on higher temperature, salinity, POC, and PON, lower pH and C:N ratios, and shallower depths compared to the other sites (Fig. 4). The second principal component (PC2) accounted for an additional 16% of the variance and was primarily driven by $\delta^{13}\text{C}$ and $\delta^{15}\text{N}$, which were negatively correlated with each other, and precipitation, which was positively correlated with $\delta^{15}\text{N}$ (Fig. 4).

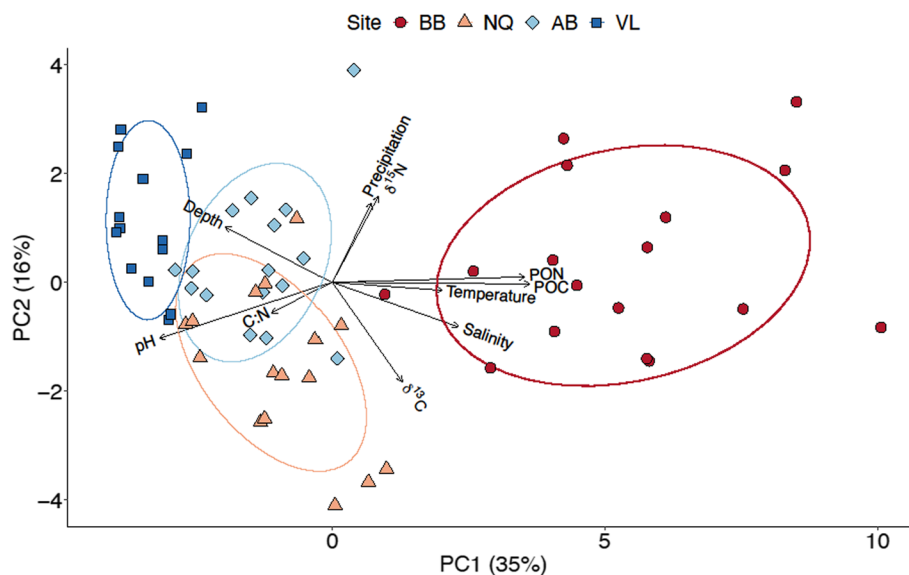


Fig. 4 Principal component analysis of the parameters: Total depth, Temperature, Salinity, pH, Precipitation, C:N ratio, Particulate organic carbon (POC), Particulate organic nitrogen (PON), Carbon stable isotope ($\delta^{13}\text{C}$), and Nitrogen stable isotope ($\delta^{15}\text{N}$). Clusters of shapes with different colors represent sampling stations: red circles indicate the Bioluminescent Bay (BB) sampling station, the orange triangles indicate the Cayo Enrique (NQ) sampling station, the light blue diamond indicate the Acidification Buoy (AB) sampling sta-

tion, and the dark blue squares indicate the Veril (VL) sampling station. The length of the vectors (lines) show the strength of their effect over each principal component. Vectors pointing in similar directions indicate positively correlated variables, vectors pointing in opposite directions indicate negatively correlated variables, and vectors at approximately right angles indicate low or no correlation. Ellipses indicate 95% confidence intervals of samples clustering within the ellipse for each station

Discussion

We observed persistently warmer, more acidic, and higher particulate organic matter conditions year-round at the inshore sites compared to sites further offshore (Figs. 2, 3, 4) likely due to a combination of differences in bathymetry, depth, flow rates, detrital material, and benthic community composition among sites (Hofmann et al. 2011; Anderson and MacKenzie 2012; Drupp et al. 2013; Page et al. 2019) (Table 2). For example, the most extreme seawater conditions in this study were observed in the shallow, inshore Bioluminescent Bay and were distinctly different from the more offshore sites (Fig. 4). We hypothesize that the semi-enclosed geomorphology of the Bioluminescent Bay presumably limited seawater exchange, while limited freshwater inputs and continued evaporation generated higher salinities (García-Troche et al. 2021) and a high biomass of seagrasses and mangroves generated substantial biogeochemical modification of seawater in the bay compared to the other sites (Figs. 2, 3, and 4). Conversely, less detectable differences in seawater parameters were observed between the more offshore Acidification Buoy and Veril sites (Figs. 2, 3, and 4), which were characterized by more open seawater exchange with offshore waters. Higher chlorophyll-*a* and turbidity were previously measured at inshore sites relative to offshore sites by sensors deployed across LPNR by Otero and Carbery (2005) suggesting these patterns of elevated nearshore organic matter may be a consistent feature of LPNR. On a smaller spatial scale, warmer and less acidic waters were observed at the shallow Cayo Enrique station relative to the Acidification Buoy station (Figs. 2, 3). This smaller spatial scale variability between these two stations located just ~150 m across the shallow reef flat (Fig. 1B) is likely due to the very shallow reef flat between the stations that led to a high degree of biogeochemical modification. Similar daytime higher temperatures and elevated pH were observed over a carbonate sediment sandbar in Kāneʻohe Bay, Hawaiʻi suggesting warming driven by daytime solar insolation and pH buffering by CaCO₃ dissolution could be common features of shallow carbonate sands of coral reef environments (Page et al. 2019). The benthos of the Cayo Enrique station was also dominated by seagrasses, which

would have further increased sampled seawater pH owing to net daytime photosynthesis (Bergstrom et al. 2019). However, the degree to which we are measuring the biogeochemical memory of seawater modification by the shallow reef flat vs the localized biogeochemical modification by the seagrass bed would require more in depth hydrodynamical studies coupled with higher frequency measurements in future studies.

This small-scale spatial variability over the shallow reef flat highlights the importance of depth, with increasing biogeochemical modification of overlying seawater typically observed for decreasing depths (Cyronak et al. 2019). Conversely, water column processes can become increasingly important drivers of coral reef seawater biogeochemistry, especially for deeper coral reef sites, and warrants additional consideration in future studies to better elucidate the relative contribution of benthic and water column processes on coral reef biogeochemistry (Long et al. 2019; Pezner et al. 2021). Collectively, these inshore–offshore differences in measured seawater parameters between sites highlight a combination of biological and physical factors as drivers of seawater chemistry with biological drivers primarily influencing the direction of biogeochemical modification while hydrodynamics primarily controlled the magnitude of biogeochemical modification (Lowe and Falter 2015; Page et al. 2019; Rintoul et al. 2022).

Limited temporal variability was observed for most of the parameters except for temperature, salinity, and pH (Fig. 2). Seawater temperatures followed expected patterns in seasonal insolation with the warmest waters observed in late summer and the coolest waters observed in late winter (Fig. 2A). Similarly, salinity followed expected declines associated with the local wet season from August to November and seasonal freshwater influxes from the distal Orinoco River (Corredor and Morell 2001) (Fig. 2B). Seawater pH was slightly reduced during the late fall when seawater temperatures were warmer, and salinities were lower (Fig. 2D). This pH variability was enhanced at the Bioluminescent Bay site during the wet season (Fig. 2D), which was also characterized by high values of particulate organic matter (Fig. 2E, F). Previous studies have suggested that temporal increases in heterotrophy of organic matter reduced seawater pH

Table 2 Mean ± standard deviation for all sampled parameters are reported for each sampling station

Site	Depth (m)	Temperature (°C)	Salinity	pH	POC (mg/m ³)	PON (mg/m ³)	C:N	δ ¹³ C (‰)	δ ¹⁵ N (‰)
BB	4.5	29 ± 1	36.4 ± 0.7	7.76 ± 0.13	432 ± 160	72 ± 32	6 ± 1	-21 ± 2.5 ± 2	
NQ	4	28 ± 1	35.3 ± 0.6	8.06 ± 0.05	134 ± 85	16 ± 5	8 ± 3	-18 ± 4.4 ± 2	
AB	6	28 ± 1	35.2 ± 0.8	7.99 ± 0.03	114 ± 27	15 ± 3	7 ± 1	-23 ± 2.5 ± 2	
VL	25	28 ± 1	35.3 ± 0.6	8.01 ± 0.03	85 ± 35	11 ± 4	8 ± 3	-24 ± 1.4 ± 3	

BB Bioluminescent Bay sampling station, NQ Cayo Enrique sampling station, AB Acidification Buoy sampling station, VL Veril sampling station

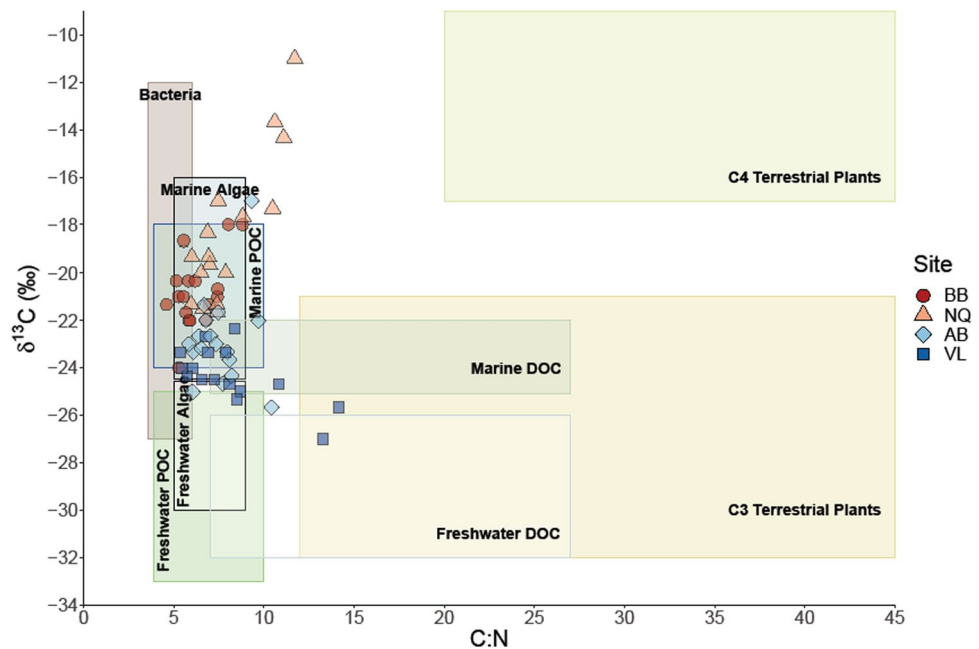
within the Bioluminescent Bay (García-Troche et al. 2021) and net heterotrophy and CaCO_3 dissolution, which decrease and increase seawater pH, respectively, were the dominant metabolic processes at the Acidification Buoy site from late spring to fall (Meléndez et al. 2022). While the primary wet season is from August to November, additional spring showers are typical in April and May and coincided with a similar decline in seawater pH and increase in particulate organic matter at the Bioluminescent Bay station (Fig. 2C–F). In contrast, there was no consistent, detectable temporal variability in seawater POC and PON outside of Bioluminescent Bay although some higher frequency variability in these parameters was recorded (Fig. 2E, F). Given the monthly sampling regime limitation, we were unable to determine any potential drivers of this higher frequency POC and PON variability. However, previous short-term deployments of sensors measuring turbidity and chlorophyll-*a* every 10 min recorded substantial high frequency variability within and between sites in LPNR (Otero and Carbery 2005). Future studies should therefore conduct higher frequency measurements of particulate organic matter and phytoplankton biomass coupled with their potential environmental drivers to determine possible drivers for POC and PON temporal variability in LPNR. Comparing diel changes in temperature, salinity and pH across sites would also provide insightful information and increase our understanding of LPNR ecosystem dynamics.

Elevated nearshore particulate organic matter (Figs. 2, 3) highlights mangroves and seagrasses as potentially important functional links of nutrition export to offshore coral ecosystems (Odum 1968; Odum et al. 1979; Lee 1995; Alldredge et al. 2013; Skinner et al. 2022). The LPNR coastline and in particular the Bioluminescent Bay is lined with mangrove forests (Fig. 1), which typically export up to 50% of organic matter produced to coastal oceans, of which 10–11% is in the form of POC (Alongi 2014; Vega Rodríguez and Aponte 2008). In LPNR, tidal particulate organic matter exports of $1.1 \text{ g C/m}^2/\text{d}$ have been measured from red mangrove (*Rhizophora mangle*) forests (Golley et al. 1962); however, more recent measurements would be needed to determine whether this export has remained constant under ongoing climate change, land-use change, and hurricane impacts. Previous sediment traps in LPNR revealed a similar range of $\delta^{13}\text{C}$ (–19.62 to –16.12‰) and $\delta^{15}\text{N}$ (1.38–3.46‰), concluding that most of the sinking particulate organic matter originated from an autochthonous mixture of algae and seagrass with generally minimal terrestrial inputs that increased closer to shore (Otero 2009). We generally observed inshore enrichment of $\delta^{13}\text{C}$ at the Bioluminescent Bay and Cayo Enrique sites (Fig. 3G), which was similar to patterns of coastal enrichment of $\delta^{13}\text{C}$ observed in the Florida Keys (Lamb and Swart 2008). Similarly, $\delta^{15}\text{N}$ was more enriched at the inshore Bioluminescent Bay site; however, there was greater

within site variability and differences between inshore and offshore sites were not as consistent as with $\delta^{13}\text{C}$ (Fig. 3H), which also coincides with patterns observed for $\delta^{15}\text{N}$ in the Florida Keys by Lamb & Swart (2008). Additionally, the PCA revealed a positive correlation between precipitation and $\delta^{15}\text{N}$ (Fig. 4) and there was a significant interaction between site and month, suggesting surface runoff following rain events is a likely source of particulate organic matter to LPNR. This pattern was particularly apparent for the Bioluminescent Bay site (Fig. 2), which had the greatest variability in $\delta^{15}\text{N}$ and is most directly impacted by coastal runoff owing to its semi-enclosed geomorphology and proximity to the shoreline. Although the initial evidence suggests that elevated inshore POC, PON, $\delta^{13}\text{C}$, and $\delta^{15}\text{N}$ (Figs. 2, 3) were related to outwelled particulate organic matter from the coastal mangroves of LPNR, the $\delta^{13}\text{C}_{\text{mean}} = -21.3\text{‰}$, $\delta^{15}\text{N}_{\text{mean}} = 4.7\text{‰}$, and $\text{C:N}_{\text{mean}} = 7.52$ indicate a mixture of primarily marine allochthonous and autochthonous organic matter (i.e., bacteria, phytoplankton, zooplankton, detrital matter, terrestrial plant material, and marine algae) as opposed to a single source (Fig. 5) (Lamb et al. 2006; Lamb and Swart 2008).

One potential explanation for particulate organic matter $\delta^{13}\text{C}$ and $\delta^{15}\text{N}$ representing a mixture of organic matter sources is that the Bioluminescent Bay is surrounded by mangroves, patched by seagrasses, and tidally flushed by marine waters. Additionally, phytoplankton $\delta^{13}\text{C}$ values can become enriched relative to the open ocean in regions with high autochthonous production, depending on the availability of carbon dioxide (CO_2) in the system and the ability of the phytoplankton to uptake bicarbonate (HCO_3^-) (Oczkowski et al. 2008, 2014). The Bioluminescent Bay is famous for large abundances of bioluminescent phytoplankton (Margalef 1961; Soler-Figueroa and Otero 2015), suggesting a high degree of autochthonous production is likely to enrich $\delta^{13}\text{C}$ in the bay. The limited exchange of seawater through the mouth of the Bioluminescent Bay could also generate a high degree of internal organic matter recycling and subsequently, further modification of $\delta^{13}\text{C}$ and $\delta^{15}\text{N}$ before export. We also observed enriched $\delta^{13}\text{C}$ and depleted $\delta^{15}\text{N}$ at the seagrass dominated Cayo Enrique site, which are typical indicators of seagrass productivity (Skinner et al. 2022). This simultaneous enrichment of $\delta^{13}\text{C}$ and depletion of $\delta^{15}\text{N}$ by seagrasses could also explain the inverse correlation between $\delta^{13}\text{C}$ and $\delta^{15}\text{N}$ in the PCA from this study (Fig. 4). Additionally, pelagic *Sargassum* spp. influxes into LPNR have been increasing since 2011, with fresh sargassum, decomposing sargassum, and sargassum brown tides observed during our sampling period that likely contributed seasonally to organic material in LPNR (Hernández et al. 2022; Pérez-Pérez 2022; León-Pérez et al. 2023). However, pelagic *Sargassum* spp. $\delta^{15}\text{N}$ from Mexico (range = –2.8 to –0.3‰; (Cabanillas-Teran et al.

Fig. 5 $\delta^{13}\text{C}$ and C:N ratio of organic matter across the study area superimposed on typical organic sources in coastal ecosystems. “BB” indicates the Bioluminescent Bay sampling station, “NQ” indicates the Cayo Enrique sampling station, “AB” indicates the Acidification Buoy sampling station, and “VL” indicates the Veril sampling station. The typical $\delta^{13}\text{C}$ and C:N ratio of organic matter for the respective source are adapted from Lamb et al. (2006)



2019) was substantially lower than the $\delta^{15}\text{N}$ observed in this study (range = 1.4–11.5‰). This suggests the leachates of decaying *Sargassum* spp. mats either had a limited impact on overall particulate organic matter export in LPNR or were fractionated upon remineralization. Collectively, it therefore appears most likely that the particulate organic matter in LPNR represents a combination of mangrove, seagrass, and marine sources and was subsequently modified by local-scale biogeochemical processes and mixing with offshore seawaters, resulting in a potential functional link of energy transfer in the form of particulate organic matter dispersal across the coastal ecosystems of LPNR.

The shallow, nearshore waters of the Bioluminescent Bay in this study were also associated with local amplification of warming and acidification (Fig. 4), suggesting that any potential benefits of particulate organic matter inputs must offset this local nearshore intensification of global-scale ocean warming and acidification. Coral heterotrophy can ameliorate post-bleaching coral stress (Grottoli et al. 2006; Houlbrèque and Ferrier-Pagès 2009; Levas et al. 2016) and maintain coral calcification under reduced seawater pH (Houlbrèque and Ferrier-Pagès 2009; Kealoha et al. 2019) suggesting the continued supply of organic matter is an important factor that modulates coral reef resistance and resilience under the climate crisis. While outwelled organic matter is often detrital with refractory components and limited bioavailability (Hemminga et al. 1994; Schlacher et al. 2009; Bainbridge et al. 2018), corals can assimilate nitrogen from a wide range of detrital organic matter and benthic sediments suggesting that organic matter, regardless of quality, is likely an available source of nitrogen for reef-building corals (Mills and Sebens 2004; Mills et al.

2004; Houlbrèque and Ferrier-Pagès 2009). We therefore hypothesize that the covariation of local amplification of warming and acidification coupled with elevated organic matter driven by the intersection of coastal geomorphology, hydrology, and functional links between mangrove, seagrass, and coral ecosystems observed in this study may also apply to other nearshore tropical reef systems. Similar inshore–offshore gradients of temperature and chlorophyll-*a* have been associated with potential coral reef refugia composed of stress-tolerant and weedy corals under ongoing environmental change across the Belize Barrier Reef System (Baumann et al. 2016). Moreover, numerous studies have suggested nearshore regions with high light attenuation may confer coral resilience to climate change, which could be partly due to elevated available coral nutrition (Sully and van Woesik 2020; Elahi et al. 2022). Further studies should assess in situ patterns of coral heterotrophy with respect to nearshore localized intensification of warming and acidification to better understand how the covariation of these drivers may confer resilience (or not) to nearshore and coastal coral communities. As mangroves and seagrasses continue to decline globally (FAO 2007; Waycott et al. 2009), this supply of organic matter may subsequently diminish and reduce the resiliency of nearshore coral reef systems dependent on outwelling from mangroves and seagrasses. Conversely, the recent influx of *Sargassum* spp. to the coastal regions of the Caribbean could be an important source of nearshore organic matter, acidification, and hypoxia that warrants further investigation for its impacts on nearshore coral reef communities (van Tussenbroek et al. 2017; Cabanillas-Teran et al. 2019; Hernández et al. 2022; Pérez-Pérez 2022; León-Pérez et al. 2023).

Mangroves and seagrasses are important drivers of the biogeochemical processes within nearshore coral reef ecosystems and the functional linkages between these systems are likely important for nearshore multi-ecosystem resilience with numerous synergistic benefits for coastal ecosystem services and communities (Harborne et al. 2006). Because the co-benefits of these coupled mangrove, seagrass, and coral ecosystems can be greater than the services provided by each of these systems individually (Guannel et al. 2016), there should be additional efforts to better understand the functional linkages that exist between them and how these may change under ongoing local and global-scale disturbances. Regardless, an expanded emphasis on conserving mangrove, seagrass, and coral reefs as coupled ecosystems to preserve their functional links will likely be of great importance within LPNR and across global tropical coastal regions to maintain essential support and ecosystem services to adjacent coastal communities.

Acknowledgements We thank the Caribbean Coastal Ocean Observing System (CARICOOS) for funding and logistical support throughout the project. We also thank Luis Rodríguez, Camille Berrocal, Khrystall Ramos, and Yeidee Alvarado for their help during special sampling events. CM-R was supported by the National Oceanic and Atmospheric Administration, Office of Education Educational Partnership Program award NA16SEC4810006-NCAS-M granted to RAA. All data and code are publicly available on *Zenodo* via <https://doi.org/10.5281/zenodo.8360492>. We thank two anonymous reviewers for their detailed and constructive feedback that greatly improved the manuscript.

Declarations

Conflict of interest The authors have no competing interests to declare that are relevant to the content of this article. The views expressed in this article are those of the authors and do not necessarily represent the views or policies of the US Environmental Protection Agency. Any mention of trade names, products, or services does not imply an endorsement by the US Government or the US Environmental Protection Agency. The EPA does not endorse any commercial products, services, or enterprises. EPA equipment was used for this research, but EPA did not operate or perform the analysis with the associated equipment. The research presented was not performed or funded by EPA and was not subject to EPA's quality system requirements.

References

- Allredge AL, Carlson CA, Carpenter RC (2013) Sources of organic carbon to coral reef flats. *Oceanography* 26:108–113
- Almodovar LR, Blomquist HL (1959) The benthic algae of Bahia Fosforescente, Puerto Rico. *Florida Academy of Sciences* 22:163–168
- Alongi DM (2014) Carbon cycling and storage in mangrove forests. *Ann Rev Mar Sci* 6:195–219
- Anderson WT, Fourqurean JW (2003) Intra- and interannual variability in seagrass carbon and nitrogen stable isotopes from south Florida, a preliminary study. *Org Geochem* 34:185–194
- Andersson AJ, MacKenzie FT (2012) Revisiting four scientific debates in ocean acidification research. *Biogeosciences* 9:893–905
- Arias PA, Bellouin N, Coppola E, Jones RG, Krinner G, Marotzke J, Naik V, Palmer MD, Plattner GK, Rogelj J, Rojas M, Sillmann J, Storelmo T, Thorne PW, Trewin B, Achuta Rao K, Adhikary B, Allan RP, Armour K, Bala G, Barimalala R, Berger S, Canadell JG, Cassou C, Cherchi A, Collins W, Collins WD, Connors SL, Corti S, Cruz F, Dentener FJ, Dercozynski C, Di Luca A, Diongue Niang A, Doblas-Reyes FJ, Dosio A, Douville H, Engelbrecht F, Eyring V, Fischer E, Forster P, Fox-Kemper B, Fuglestedt JS, Fyfe JC, Gillett NP, Goldfarb L, Gorodetskaya I, Gutierrez JM, Hamdi R, Hawkins E, Hewitt HT, Hope P, Islam AS, Jones C, Kaufman DS, Kopp RE, Kosaka Y, Kossin J, Krakovska S, Lee JY (2021) Technical Summary in *Climate Change 2021: The Physical Science Basis. Contribution of Working Group I to the Sixth Assessment Report of the Intergovernmental Panel on Climate Change*.
- Ayala-Torres R (2022) Seasonal dissolved oxygen fluctuations through the water column in a shallow tropical bioluminescent bay, La Parguera, Lajas. Master Thesis, University of Puerto Rico Mayaguez
- Bainbridge Z, Lewis S, Bartley R, Fabricius K, Collier C, Waterhouse J, Garzon-Garcia A, Robson B, Burton J, Wenger A, Brodie J (2018) Fine sediment and particulate organic matter: A review and case study on ridge-to-reef transport, transformations, and impacts on marine ecosystems. *Mar Pollut Bull* 135:1205–1220
- Baumann JH, Townsend JE, Courtney TA, Aichelman HE, Davies SW, Lima FP, Castillo KD (2016) Temperature regimes impact coral assemblages along environmental gradients on lagoonal reefs in Belize. *PLoS One* 11
- Bergstrom E, Silva J, Martins C, Horta P (2019) Seagrass can mitigate negative ocean acidification effects on calcifying algae. *Sci Rep* 9:
- Bianchi TS, Bauer JE (2011) Particulate organic carbon cycling and transformation. *Treatise on Estuarine and Coastal Science*. pp 69–117
- Bouillon S, Connolly RM (2009) Carbon exchange among tropical coastal ecosystems. In: Nagelkerken I (ed) *Ecological Connectivity among Tropical Coastal Ecosystems*. Springer Science and Business Media, pp 45–70
- Brian F (2006) *Stable isotope ecology*. Springer
- Cabanillas-Teran N, Hernandez-Arana HA, Ruiz-Zarate MA, Vega-Zepeda A, Sanchez-Gonzalez A (2019) Sargassum blooms in the Caribbean alter the trophic structure of the sea urchin *Diadema antillarum*. *PeerJ* 7:e7589
- Cael BB, Follows MJ (2016) On the temperature dependence of oceanic export efficiency. *Geophys Res Lett* 43:5170–5175
- Chaves JE, Cetinić I, Dall'Olmo G, Estapa M, Gardner W, Goñi M, Graff JR, Hernes P, Lam PJ, Liu Z, Lomas MW, Mannino A, Novak MG, Turnewitsch R, Werdell PJ, Westberry TK (2020) Particulate organic carbon sampling and measurement protocols: consensus towards future ocean color missions.
- Corredor JE, Morell JM (2001) Seasonal variation of physical and biogeochemical features in eastern Caribbean Surface Water. *J Geophys Res Oceans* 106:4517–4525
- Courtney TA, Lebrato M, Bates NR, Collins A, De Putron SJ, Garley R, Johnson R, Molinero J-C, Noyes TJ, Sabine CL, Andersson AJ (2017) Environmental controls on modern scleractinian coral and reef-scale calcification. *Sciences Advances* 3:e1701356
- Courtney TA, Kindeberg T, Andersson AJ (2020) Coral calcification responses to the North Atlantic Oscillation and coral bleaching in Bermuda. *PLoS One* 15
- Cruz BN, Neuer S (2019) Heterotrophic bacteria enhance the aggregation of the marine picocyanobacteria *prochlorococcus* and *synchococcus*. *Front Microbiol* 10:

- Cyronak T, Takeshita Y, Courtney TA, DeCarlo EH, Eyre BD, Kline DI, Martz T, Page H, Price NN, Smith J, Stoltenberg L, Tresguerres M, Andersson AJ (2019) Diel temperature and pH variability scale with depth across diverse coral reef habitats. *Limnol Oceanogr Lett* 5:193–203
- Dawson TE, Brooks PD (2001) Fundamentals of stable isotope chemistry and measurement. *Stable Isotope Techniques in the Study of Biological Processes and Functioning of Ecosystems*. pp 1–28
- Diaz RJ (2001) Overview of Hypoxia around the World 30:275–281
- Dickson AG (Andrew G, Sabine CL, Christian JR (2007) Guide to best practices for ocean CO₂ measurements.
- Doney SC (2010) The growing human footprint on coastal and open-Ocean biogeochemistry. *Science* (1979) 328:1512–1516
- Drupp PS, De Carlo EH, Mackenzie FT, Sabine CL, Feely RA, Shamberger KE (2013) Comparison of CO₂ dynamics and air-sea gas exchange in differing tropical reef environments. *Aquat Geochem* 19:371–397
- Duarte CM, Regaudie-de-Gioux A, Arrieta JM, Delgado-Huertas A, Agustí S (2013) The oligotrophic ocean is heterotrophic. *Ann Rev Mar Sci* 5:551–569
- Ducklow HW, Doney SC (2013) What is the metabolic state of the oligotrophic ocean? A debate. *Ann Rev Mar Sci* 5:525–533
- Eakin CM, Devotta D, Heron S, Connolly S, Liu G, Geiger E, De La Cour J, Gomez A, Skirving W, Baird A, Cantin N, Couch C, Donner S, Gilmour J, Gonzalez-Rivero M, Gudka M, Harrison H, Hodgson G, Hoegh-Guldberg O, Hoey A, Hoogenboom M, Hughes T, Johnson M, Kerry J, Mihaly J, Muñiz-Castillo A, Obura D, Pratchett M, Rivera-Sosa A, Ross C, Stein J, Thompson A, Torda G, Viehman TS, Walter C, Wilson S, Marsh B, Spady B, Dyer N, Adam T, Alidoostsalimi M, Alidoostsalimi P, Alvarez-Filip L, Álvarez-Noriega M, Bahr K, Barnes P, Barraza-Sandoval J, Baum J, Bauman A, Beger M, Berry K, Bessell-Browne P, Bigot L, Bonito V, Brodnicke O, Burdick D, Burkepile D, Burt A, Burt J, Butler I, Caldwell J, Chancerelle Y, Chen CA, Cherh K-L, Childress M, Coken D, Coward G, Crabbe MJ, Dallison T, Dalton S, DeCarlo T, Drury C, Drysdale I, Edwards C, Eggertsen L, Elma E, Ennis R, Evans R, Eyal G, Fenner D, Figueroa-Zavala B, Fisch J, Fox M, Gadoutsis E, Gilbert A, Halford A, Heintz T, Hewlett J, Hobbs J-PA, Hoot W, Houk P, Johnston L, Johnston M, Kayanne H, Kennedy E, Kikuchi R, Kloiber U, Koike H, Kramer L, Kuo C-Y, Lang J, Leadbeater A, Leão Z, Lee J, Lewis C, Lirman D, Longo G, MacDonald C, Mangubhai S, Da Silva I, Mason-Parker C, McDonough V, McField M, Mello T, Mithernique - Agathe C, Moldzio S, Monroe A, Montefalcone M, Moses K, Mostafavi PG, Moura R, Munasinghe C, Nakamura T, Nicet J-B, Nuttall M, Oliveira M, Oxenford H, Pandolfi J, Patankar V, Perez D, Perera N, Prabuning D, Precht W, Raj KD, Reimer J, Richardson L, Rotjan R, Ryan N, Salm R, Sandin S, Schopmeyer S, Shokri M, Smith J, Smith K, Smith SR, Smith T, Sommer B, Soto M, Sykes H, Tagarino K, Teoh M, Thai M, Toh T, Tredinnick A, Tso A, Tyley H, Ussi A, Vaterlaus C, Vermeij M, Vo ST, Voolstra C, Wee HB, Weiler B, Yahya S, Yeemin T, Ziegler M, Kimura T, Manzello D (2022) The 2014–17 global coral bleaching event: the most severe and widespread coral reef destruction.
- Eddy TD, Lam VWY, Reygondeau G, Cisneros-Montemayor AM, Greer K, Palomares MLD, Bruno JF, Ota Y, Cheung WWL (2021) Global decline in capacity of coral reefs to provide ecosystem services. *One Earth* 4:1278–1285
- Elahi R, Edmunds PJ, Gates RD, Kuffner IB, Barnes BB, Chollett I, Courtney TA, Guest JR, Lenz EA, Toth LT, Viehman TS, Williams ID (2022) Scale dependence of coral reef oases and their environmental correlates. *Ecological Applications* 32
- FAO (2007) *World's Mangroves 1980–2005*. FAO, Rome
- García-Sais J, Appeldoorn R, Battista T, Bauer L, Bruckner A, Caldwell C, Carrubba L, Corredor J, Diaz E, Lilyestrom C, García-Moliner G, Hernández-Delgado E, Menza C, Morell J, Pait A, Sabater J, Weil E, Williams E, Williams S (2021) *The State of Coral Reef Ecosystems of Puerto Rico*.
- García-Troche EM, Morell JM, Meléndez M, Salisbury JE (2021) Carbonate chemistry seasonality in a tropical mangrove lagoon in La Parguera, Puerto Rico. *PLoS One* 16
- Golley F, Odum HT, Wilson RF (1962) The Structure and Metabolism of a Puerto Rican Red Mangrove Forest in May. Source: *Ecology* 43
- Goreau TF, Goreau NI, Yonge CM (1971) Reef Corals: autotrophs or heterotrophs? *Biology Bulletin* 141:247–260
- Grottoli AG, Rodrigues LJ, Palardy JE (2006) Heterotrophic plasticity and resilience in bleached corals. *Nature* 440:1186–1189
- Guannel G, Arkema K, Ruggiero P, Verutes G (2016) The power of three: coral reefs, seagrasses and mangroves protect coastal regions and increase their resilience. *PLoS One* 11
- Harborne AR, Mumby PJ, Micheli F, Perry CT, Dahlgren CP, Holmes KE, Brumbaugh DR (2006) The functional value of Caribbean coral reef, seagrass and mangrove habitats to ecosystem processes. *Adv Mar Biol* 50:57–189
- Hatcher BG (1988) Coral reef primary productivity: A Beggar's banquet. *TREE* 3:106–111
- Hemminga MA, Slim FJ, Kazungu J, Ganssen GM, Nieuwenhuize J, Kruyt NM (1994) Carbon outwelling from a mangrove forest with adjacent seagrass beds and coral reefs (Gazi Bay, Kenya). *Marine Ecology and Progress Series* 106:291–301
- Hernández WJ, Morell JM, Armstrong RA (2022) Using high-resolution satellite imagery to assess the impact of Sargassum inundation on coastal areas. *Remote Sensing Letters* 13:24–34
- Hernández-López WJ (2015) Benthic habitat mapping and bio-optical characterization La Parguera Marine Reserve using passive and active remote sensing data. Universidad de Puerto Rico, PhD
- Hoegh-Guldberg O, Bruna JF (2010) The impact of climate change on the world's marine ecosystems. *Science* (1979) 328:1523–1528
- Hofmann GE, Smith JE, Johnson KS, Send U, Levin LA, Micheli F, Paytan A, Price NN, Peterson B, Takeshita Y, Matson PG, de Crook E, Kroeker KJ, Gambi MC, Rivest EB, Frieder CA, Yu PC, Martz TR (2011) High-frequency dynamics of ocean pH: A multi-ecosystem comparison. *PLoS One* 6
- Houlbrèque F, Ferrier-Pagès C (2009) Heterotrophy in tropical scleractinian corals. *Biol Rev* 84:1–17
- Kałędkowski D (2023) Running Operations for Vectors Package (<<https://orcid.org/0000-0001-9533-457X>>)
- Kealoha AK, Shamberger KEF, Reid EC, Davis KA, Lentz SJ, Brainard RE, Oliver TA, Rappé MS, Roark EB, Rii YM (2019) Heterotrophy of oceanic particulate organic matter elevates net ecosystem calcification. *Geophys Res Lett* 46:9851–9860
- Kharbush JJ, Close HG, Van Mooy BAS, Arnosti C, Smittenberg RH, Le Moigne FAC, Mollenhauer G, Scholz-Böttcher B, Obrecht I, Koch BP, Becker KW, Iversen MH, Mohr W (2020) Particulate organic carbon deconstructed: molecular and chemical composition of particulate organic carbon in the ocean. *Front Mar Sci* 7
- Knap A, Michaels A, Close A, Ducklow H, Dickson A (1996) Protocols for the Joint Global Ocean Flux Study (JGOS) core measurements. *JGOS Report Nr 19*, vi+170 pp
- Lamb K, Swart PK (2008) The carbon and nitrogen isotopic values of particulate organic material from the Florida Keys: A temporal and spatial study. *Coral Reefs* 27:351–362
- Lamb A, Wilson GP, Leng MJ (2006) A review of coastal palaeoclimate and relative sea-level reconstructions using $\delta^{13}C$ and C/N ratios in organic material. *Earth Sci Rev* 75:29–57
- Lee SY (1995) Mangrove outwelling: a review. *Hydrobiologia* 295:203–212
- León-Pérez MC, Reisinger AS, Gibeau JC (2023) Spatial-temporal dynamics of decaying stages of pelagic Sargassum spp. along

- shorelines in Puerto Rico using Google Earth Engine. *Mar Pollut Bull* 188
- Levas S, Grottolli AG, Schoepf V, Aschaffenburg M, Baumann J, Bauer JE, Warner ME (2016) Can heterotrophic uptake of dissolved organic carbon and zooplankton mitigate carbon budget deficits in annually bleached corals? *Coral Reefs* 35:495–506
- Long MH, Rheuban JE, McCorkle DC, Burdige DJ, Zimmerman RC (2019) Closing the oxygen mass balance in shallow coastal ecosystems. *Limnol Oceanogr* 64:2694–2708
- Lowe RJ, Falter JL (2015) Oceanic forcing of coral reefs. *Ann Rev Mar Sci* 7:43–66
- Lüdecke et al (2021) performance: An R Package for Assessment, Comparison and Testing of Statistical Models. *Journal of Open-Source Software* 6(60):3139. <https://doi.org/10.21105/joss.03139>
- Luijendijk E, Gleeson T, Moosdorf N (2020) Fresh groundwater discharge insignificant for the world's oceans but important for coastal ecosystems. *Nat Commun* 11
- Margalef R (1961) Hidrografía y fitoplankton de un area marina de la costa meridional de Puerto Rico. Instituto de Investigaciones Pesqueras XVIII:33–96
- Meléndez M, Salisbury J, Gledhill D, Langdon C, Morell JM, Manzello D, Sutton A (2022) Net ecosystem dissolution and respiration dominate metabolic rates at two western Atlantic reef sites. *Limnol Oceanogr* 67:527–539
- Meléndez M, Salisbury J, Gledhill D, Langdon C, Morell JM, Manzello D, Rodriguez-Abudo S, Musielewicz S, Sutton A (2020) Seasonal variations of carbonate chemistry at two Western Atlantic coral reefs. *J Geophys Res Oceans* 125
- Mills MM, Sebens KP (2004) Ingestion and assimilation of nitrogen from benthic sediments by three species of coral. *Mar Biol* 145:1097–1106
- Mills MM, Lipschultz F, Sebens KP (2004) Particulate matter ingestion and associated nitrogen uptake by four species of scleractinian corals. *Coral Reefs* 23:311–323
- Mishonov A V, Gardner WD, Richardson MJ (2003) Remote sensing and surface POC concentration in the South Atlantic. *Deep Sea Res* 2 Top Stud Oceanogr 50:2997–3015
- Moberg F, Folke C (1999) Ecological goods and services of coral reef ecosystems. *Ecol Econ* 29:215–233
- Morelock J, Schneidermann N, Bryant WR (1977) Shelf reefs, southwestern Puerto Rico. Reefs and related carbonates—ecology and sedimentology. *Studies in Geology* 4:17–25
- Oczkowski A, Nixon S, Henry K, DiMilla P, Pilson M, Granger S, Buckley B, Thornber C, McKinney R, Chaves J (2008) Distribution and trophic importance of anthropogenic nitrogen in Narragansett Bay: An assessment using stable isotopes. *Estuaries Coasts* 31:53–69
- Oczkowski A, Markham E, Hanson A, Wigand C (2014) Carbon stable isotopes as indicators of coastal eutrophication. *Ecol Appl* 24:457–466
- Oczkowski A, Kreakie B, McKinney RA, Prezioso J (2016) Patterns in stable isotope values of nitrogen and carbon in particulate matter from the northwest Atlantic continental shelf, from the gulf of Maine to Cape Hatteras. *Front Mar Sci* 3
- Oczkowski A, Taplin B, Pruell R, Pimenta A, Johnson R, Grear J (2018) Carbon stable isotope values in plankton and mussels reflect changes in carbonate chemistry associated with nutrient enhanced net production. *Front Mar Sci* 5
- Odum EP (1968) Energy flow in ecosystems: A historical review. *Integr Comp Biol* 8:11–18
- Odum WE, Fisher JS, Pickral JC (1979) Factors controlling the flux of organic carbon from estuarine wetlands. *Ecological Processes in Coastal and Marine Systems*
- Otero E (2009) Spatial and temporal patterns of water quality indicators in reef systems of southwestern Puerto Rico. *Caribb J Sci* 45:168–180
- Otero E, Carbery KK (2005) Chlorophyll-a and turbidity patterns over coral reefs systems of La Parguera Natural Reserve, Puerto Rico. *Int J Trop Biol* 53:25–32
- Page HN, Courtney TA, De Carlo EH, Howins NM, Koester I, Andersson AJ (2019) Spatiotemporal variability in seawater carbon chemistry for a coral reef flat in Kāneʻohe Bay, Hawaiʻi. *Limnol Oceanogr* 64:913–934
- Paul D, Skrzypek G, Fórizs I (2007) Normalization of measured stable isotopic compositions to isotope reference scales - A review. *Rapid Commun Mass Spectrom* 21:3006–3014
- Pérez-Pérez J (2022) Impacts of floating Sargassum accumulation on the fringing mangrove *Rhizophora mangle* in Southwestern Puerto Rico: A case study. University of Puerto Rico, Master's
- Pezner AK, Courtney TA, Page HN, Giddings SN, Beatty CM, DeGrandpre MD, Andersson AJ (2021) Lateral, vertical, and temporal variability of seawater carbonate chemistry at Hog Reef, Bermuda. *Front Mar Sci* 8
- R Core Team (2022) R: A language and environment for statistical computing. R Foundation for Statistical Computing, Vienna, Austria. URL <https://www.R-project.org/>.
- Ramajo L, Pérez-León E, Hendriks IE, Marbà N, Krause-Jensen D, Sejr MK, Blicher ME, Lagos NA, Olsen YS, Duarte CM (2016) Food supply confers calcifiers resistance to ocean acidification. *Sci Rep* 6
- Rezende CE, Lacerda LD, Ovalle ARC, Silva CAR, Martinelli LA (1990) Nature of POC Transport in a Mangrove Ecosystem: A Carbon Stable Isotopic Study 30:641–645
- Rintoul MS, Courtney TA, Dohner JL, Giddings SN, Kekuwa SAH, Mitarai S, ... & Andersson AJ (2022) The effects of light intensity and flow speed on biogeochemical variability within a fringing coral reef in Onna-son, Okinawa, Japan. *Journal of Geophysical Research: Oceans*, 127(12), e2021JC018369.
- Robertson AI, Alongi DM, Boto KG (1984) Food chains and carbon fluxes. *Coastal and Estuarine Studies*. pp 293–326
- Rodelli MR, Gearing JN, Gearing PJ, Marshall N, Sasekumar A (1984) Stable isotope ratio as a tracer of mangrove carbon in Malaysian ecosystems. *Oecologia* 61:326–333
- Ryan KE, Walsh JP, Corbett DR, Winter A (2008) A record of recent change in terrestrial sedimentation in a coral-reef environment, La Parguera, Puerto Rico: A response to coastal development? *Mar Pollut Bull* 56:1177–1183
- Sale PF, Agardy T, Ainsworth CH, Feist BE, Bell JD, Christie P, Hoegh-Guldberg O, Mumby PJ, Feary DA, Saunders MI, Daw TM, Foale SJ, Levin PS, Lindeman KC, Lorenzen K, Pomeroy RS, Allison EH, Bradbury RH, Corrin J, Edwards AJ, Obura DO, Sadovy de Mitcheson YJ, Samoilys MA, Sheppard CRC (2014) Transforming management of tropical coastal seas to cope with challenges of the 21st century. *Mar Pollut Bull* 85:8–23
- Santos IR, Burdige DJ, Jennerjahn TC, Bouillon S, Cabral A, Serrano O, Wernberg T, Filbee-Dexter K, Guimond JA, Tamborski JJ (2021) The renaissance of Odum's outwelling hypothesis in "Blue Carbon" science. *Estuar Coast Shelf Sci* 255:
- Schlacher TA, Connolly RM, Skillington AJ, Gaston TF (2009) Can export of organic matter from estuaries support zooplankton in nearshore, marine plumes? *Aquat Ecol* 43:383–393
- Sherman C, Schmidt W, Appeldoorn R, Hutchinson Y, Ruiz H, Nemeth M, Bejarano I, Motta JJC, Xu H (2016) Sediment dynamics and their potential influence on insular slope mesophotic coral ecosystems. *Cont Shelf Res* 129:1–9
- Sippo JZ, Maher DT, Tait DR, Ruiz-Halpern S, Sanders CJ, Santos IR (2017) Mangrove outwelling is a significant source of oceanic exchangeable organic carbon. *Limnol Oceanogr Lett* 2:1–8

- Skinner C, Cobain MRD, Zhu Y, Wyatt ASJ, Polunin NVC (2022) Progress and direction in the use of stable isotopes to understand complex coral reef ecosystems: A Review. *Oceanogr Mar Biol Annu Rev* 60:373–432
- Soler-Figueroa BM, Otero E (2015) The influence of rain regimes and nutrient loading on the abundance of two Dinoflagellate species in a tropical bioluminescent bay, Bahía Fosforescente, La Parguera, Puerto Rico. *Estuaries Coasts* 38:84–92
- Sully S, van Woesik R (2020) Turbid reefs moderate coral bleaching under climate-related temperature stress. *Glob Chang Biol* 26:1367–1373
- Todd B, Ballantine DL, Otero E (2009) Nutrient distribution across the insular shelf of La Parguera, Puerto Rico: Assessment by algal tissue nitrogen. *Caribb J Sci* 45:181–190
- Towle EK, Enochs IC, Langdon C (2015) Threatened Caribbean coral is able to mitigate the adverse effects of ocean acidification on calcification by increasing feeding rate. *PLoS ONE* 10:1–18
- United Nations (2021) The Second World Ocean Assessment Volume II
- van Tussenbroek BI, Hernández Arana HA, Rodríguez-Martínez RE, Espinoza-Avalos J, Canizales-Flores HM, González-Godoy CE, Barba-Santos MG, Vega-Zepeda A, Collado-Vides L (2017) Severe impacts of brown tides caused by *Sargassum* spp. on near-shore Caribbean seagrass communities. *Mar Pollut Bull* 122:272–281
- Vega Rodríguez M, Aponte NE (2008) Estimating primary productivity of red mangroves in southwestern Puerto Rico from remote sensing and field measurements. Master Thesis, University of Puerto Rico
- Wang M, Hu C, Barnes BB, Mitchum G, Lapointe B, Montoya JP (2019) The great Atlantic Sargassum belt. *Science* (1979) 365:83–87
- Waycott M, Duarte CM, Carruthers TJB, Orth RJ, Dennison WC, Olyarnik S, Calladine A, Fourqurean JW, Heck KL, Hughes AR, Kendrick GA, Kenworthy WJ, Short FT, Williams SL (2009) Accelerating loss of seagrasses across the globe threatens coastal ecosystems. *PNAS* 106:12377–12381
- Williams PJB, Quay PD, Westberry TK, Behrenfeld MJ (2012) The oligotrophic ocean is autotrophic. *Ann Rev Mar Sci* 1–15
- Yeakel KL, Andersson AJ, Bates NR, Noyes TJ, Collins A, Garley R (2015) Shifts in coral reef biogeochemistry and resulting acidification linked to offshore productivity. *PNAS* 112:14512–14517
- Zayas-Santiago CC (2011) Landscape structure in two reefs in La Parguera and the distribution of the *Lytechinus variegatus*. University of Puerto Rico-Mayaguez, Master's

Publisher's Note Springer Nature remains neutral with regard to jurisdictional claims in published maps and institutional affiliations.

Springer Nature or its licensor (e.g. a society or other partner) holds exclusive rights to this article under a publishing agreement with the author(s) or other rightsholder(s); author self-archiving of the accepted manuscript version of this article is solely governed by the terms of such publishing agreement and applicable law.